

LATTICE BOLTZMANN SIMULATIONS OF DRAG REDUCTION BY SUPER-HYDROPHOBIC SURFACES

Rastegari Amirreza & Akhavan Rayhaneh

Department of Mechanical Engineering, University of Michigan, Ann Arbor, MI 48102-2125, USA

Abstract Drag reduction by super-hydrophobic surfaces is investigated using Lattice Boltzmann simulations in turbulent channel flow. The super-hydrophobic surface is modeled as longitudinal arrays of slip/no-slip stripes of size $4 \leq g^{+0} = w^{+0} \leq 128$, covering both channel walls, where g^{+0} and w^{+0} denote the widths of the slip and no-slip stripes, respectively, normalized with respect to the friction-velocity of the base flow and viscosity. An additional case was also run with $g^{+0} = 28$, $w^{+0} = 4$. All simulations were performed in channels of size $5h \times 2.5h \times 2h$ at a bulk Reynolds number of $Re_b = U_b h / \nu = 3600$ ($Re_{\tau_0} \approx 230$), where h denotes the channel half height. Drag reductions of 5%, 11%, 18%, 23%, 38%, 47% and 51% were observed for $g^{+0} = w^{+0} = 4, 8, 16, 32, 64, 128$ and $g^{+0} = 28, w^{+0} = 4$, respectively. Mathematical analysis shows that the magnitude of drag reduction can be expressed as $DR = U_s/U_b + \varepsilon$, where ε is zero in laminar flow, but attains a small non-zero value in turbulent flow proportional to the magnitude of DR. Results from both the present DNS studies as well as prior experiments [1] were found to fit this scaling. The one-point turbulence statistics show characteristics of combined slip described by [3]. When normalized in wall units, the turbulence statistics and structure remains nearly unchanged outside of a layer of thickness on the order of one slip-length from the walls. Drag reduction is found to be due to a weakening of the turbulence structures accompanied by a drop in turbulence production throughout the channel, but especially over the slip surfaces.

INTRODUCTION

Super-hydrophobic surfaces have shown promise as a means of skin-friction drag reduction in the recent years [4]. However, experimental results have been inconsistent, and two main questions regarding the scaling of drag reduction with super-hydrophobic surface properties and mechanism of drag reduction remain unanswered.

The objective of the present study is to use results from DNS in turbulent channel flow using Lattice-Boltzmann (LB) methods to further investigate these questions. The super-hydrophobic surface is modeled as longitudinal arrays of slip/no-slip stripes covering both channel walls. As such, the gas/liquid interface in the real super-hydrophobic surface is modeled as a flat shear-free interface. A schematic of the channel geometry and coordinate system is shown in figure 1. Six different cases were studied corresponding to $g^{+0} = w^{+0} = 4, 8, 16, 32, 64, 128$, where g^{+0} and w^{+0} denote width of the slip and no-slip stripes in wall units. In all of these cases fraction of shear-free to no-slip surface area was kept constant at 1 : 1. An additional case with $g^{+0} = 28$ and $w^{+0} = 4$ was also investigated. All simulations were performed in channels of size $5h \times 2.5h \times 2h$ at a constant bulk Reynolds number of $Re_b = U_b h / \nu = 3600$, corresponding to a base friction Reynolds number of $Re_{\tau_0} = u_{\tau_0} h / \nu \approx 230$, where h denotes the channel half-height. Standard D3Q19 single relaxation time Lattice Boltzmann method was used for all the simulations.

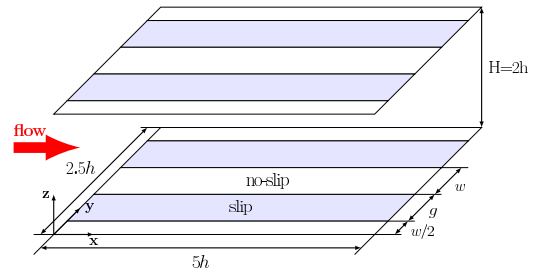


Figure 1. The channel geometry and coordinate system.

All simulations were performed in channels of size $5h \times 2.5h \times 2h$ at a constant bulk Reynolds number of $Re_b = U_b h / \nu = 3600$, corresponding to a base friction Reynolds number of $Re_{\tau_0} = u_{\tau_0} h / \nu \approx 230$, where h denotes the channel half-height. Standard D3Q19 single relaxation time Lattice Boltzmann method was used for all the simulations.

RESULTS AND DISCUSSION

Drag reductions of 5%, 11%, 18%, 23%, 38%, 47% and 51% were observed for $g^{+0} = w^{+0} \approx 4, 8, 16, 32, 64, 128$ and $w^{+0} = 4, g^{+0} = 28$, respectively. The corresponding slip velocities were $U_s/U_b = 0.06, 0.10, 0.15, 0.23, 0.32, 0.37$ and 0.45 , where U_s denotes the average slip-velocity at the wall. Mathematical analysis shows that the magnitude of drag reduction scales as $DR = U_s/U_b + \varepsilon$. This scaling is valid in both laminar and turbulent flow and is independent of the Reynolds number. The value of ε is zero in laminar flow. In turbulent flow, ε attains a small non-zero value proportional to the magnitude of drag reduction. Figure 2(a) shows the comparison of results from the present DNS in turbulent channel flow, DNS in laminar channel flow, and experiments of [1] in turbulent channel flow with the scaling $DR = U_s/U_b$. Prior studies have suggested that the magnitude of DR scales with l_s^{+0} and Re_{τ_0} [2] or with g^{+0} [5] in turbulent flow, and with $(w + g)/2H$ in laminar flow [6]. Comparison of the present DNS results in laminar and turbulent channel flow and experimental results in turbulent channel flow with these scalings, shown in Figures 2(a-c), indicates that U_s/U_b provides the best match to all the available data.

Figure 3 shows the one-point turbulence statistics in drag-reduced flow compared to the base channel with no-slip walls. The mean velocity profiles (Fig. 3b) show characteristics of combined slip described by [3]. Presence of the slip/no-slip stripes also gives rise to a mean secondary flow in the channel in the form of pairs of counter-rotating streamwise vortices. The turbulence intensities normalized in wall units (Fig. 3c) show an increase in the streamwise and spanwise components

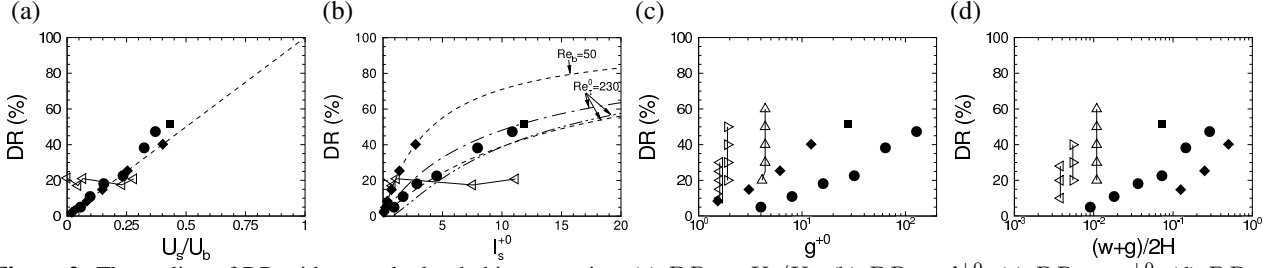


Figure 2. The scaling of DR with super-hydrophobic properties: (a) DR vs. U_s/U_b ; (b) DR vs. l_s^{+0} ; (c) DR vs. g^{+0} ; (d) DR vs. $(w+g)/2H$. \bullet , LB DNS at $Re_b = 3600$ ($Re_{\tau_0} \approx 230$) with $4 \leq g^{+0} = w^{+0} \leq 128$; \blacksquare , LB DNS at $Re_b = 3600$ ($Re_{\tau_0} \approx 230$) with $g^{+0} \approx 28, w^{+0} \approx 4$; \blacklozenge , LB DNS of laminar flow at $Re_b = 100$; \leftarrow , Experiments of [1] at $2450 \leq Re_b \leq 4000$, $g = w = 30\mu m$, micro-grooves on one wall; \rightarrow , Experiments of [1] at $1100 \leq Re_b \leq 2900$, $g = w = 30\mu m$, micro-grooves on both walls; \triangleleft , Experiments of [1] at $1500 \leq Re_b \leq 4000$, $g = w = 60\mu m$, micro-grooves on both walls; $---$, $DR = U_s/U_b = l_s^{+0}/[l_s^{+0} + (Re_b/Re_{\tau_0})]$; $- \cdot -$, Results of [2] for streamwise slip; $- \cdot \cdot -$, Results of [2] for combined slip.

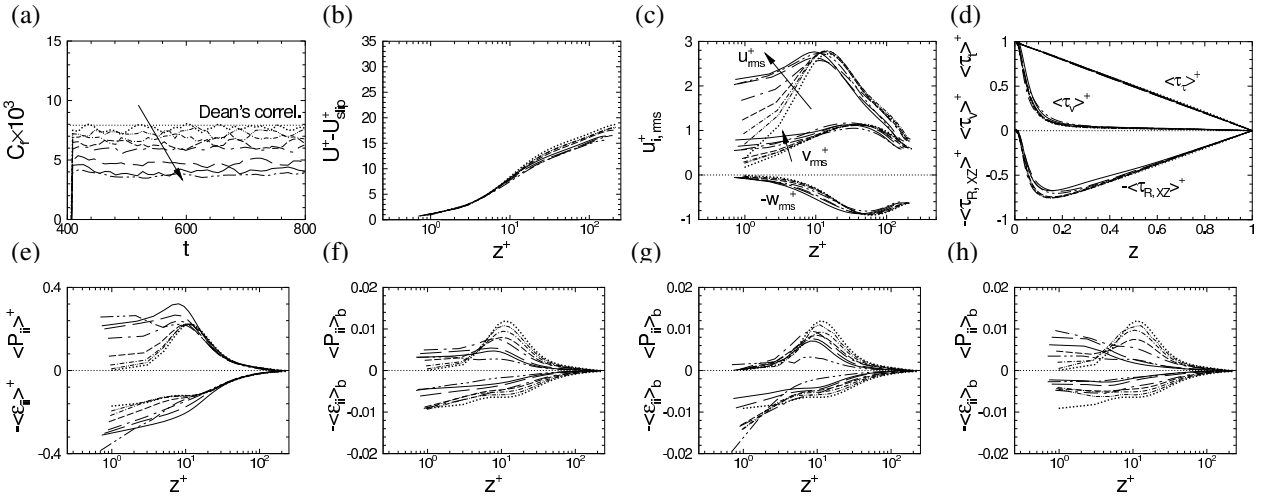


Figure 3. Turbulence statistics in drag reduced flow: (a) skin-friction coefficient, C_f ; (b) mean velocity profile; (c) turbulence intensities; (d) Reynolds shear stress $\langle \tau_{R,xz} \rangle$, viscous shear stress $\langle \tau_v \rangle$, and total stress $\langle \tau_t \rangle$; (e) TKE production and dissipation in wall units (f) TKE production and dissipation normalized with U_b and h , (g) TKE production and dissipation over the no-slip stripes in bulk units, (h) TKE production and dissipation over the slip stripes in bulk units; $- \cdot -$, LB DNS, $g^{+0} = w^{+0} \approx 4, 5\%DR$; $- \cdot \cdot -$, LB DNS, $g^{+0} = w^{+0} \approx 8, 10.9\%DR$; $---$, LB DNS, $g^{+0} = w^{+0} \approx 16, 18.2\%DR$; $- \cdot \cdot \cdot -$, LB DNS, $g^{+0} = w^{+0} \approx 32, 22.6\%DR$; $---$, LB DNS, $g^{+0} = w^{+0} \approx 64, 38.2\%DR$; $---$, LB DNS, $g^{+0} = w^{+0} \approx 128, 47.3\%DR$; $---$, LB DNS, $g^{+0} \approx 28, w^{+0} \approx 4, 51.6\%DR$; \dots , LB DNS, No-Slip channel.

up to a distance on the order of $z^+ \approx l_s^+$ from the walls. Outside of this region, the turbulence statistics are nearly the same as regular channel flow if normalized in wall units. The Reynolds shear stress (Fig. 3d), normalized in wall units, shows a drop at high DRs, reflecting the lower Reynolds number of the flow after drag reduction.

Similar trends are also observed in the Turbulence Kinetic Energy (TKE) production and dissipation, as shown in Fig. 3(e). When normalized in wall units, the production and dissipation are nearly unchanged from regular channel flow outside of a layer of thickness $z^+ \approx l_s^+$ near the walls. For $z^+ < l_s^+$, there is additional turbulence production and dissipation due to the secondary flow created by the slip/no-slip stripes. When plotted in bulk units, however, large drops in TKE production and dissipation can be observed with increasing magnitude of DR, as shown in Fig. 3(f). This drop is observed both on no-slip and slip surfaces, but is far more pronounced over the slip surfaces, as shown in Fig. 3(g-h). This drop in TKE production is believed to be the origin of DR with super-hydrophobic surfaces.

References

- [1] R. J. Daniello, N. E. Waterhouse, and J. P. Rothstein. Drag reduction in turbulent flows over superhydrophobic surfaces. *Phys. Fluids* **21**: 085103, 2009.
- [2] K. Fukagata, N. Kasagi, and P. Koumoutsakos. A theoretical prediction of friction drag reduction in turbulent flow by superhydrophobic surfaces. *Phys. Fluids* **18**: 051703, 2006.
- [3] T. Min, and J. Kim. Effect of superhydrophobic surfaces on skin-friction drag. *Phys. Fluids* **16**: L55, 2004.
- [4] J. P. Rothstein. Slip on superhydrophobic surfaces. *Annu. Rev. Fluid Mech* **42**: 89–109, 2010.
- [5] M. B. Martel, J. P. Rothstein, and J. B. Perot. An analysis of superhydrophobic turbulent drag reduction mechanisms using direct numerical simulation. *Phys. Fluids* **22**: 065102, 2010.
- [6] J. R. Philip. Integral properties of flows satisfying mixed no-slip and no-shear conditions. *J. Applied Mathematics and Physics (ZAMP)* **23**: 960–968, 1972.